Supporting Information for:

Enhancement of CO_2 Binding and Mechanical Properties Upon Diamine Functionalization of M_2(dobpdc) Metal-Organic Frameworks

Jung-Hoon Lee,[1,2] Rebecca L. Siegelman,[3] Lorenzo Maserati,[1] Tonatiuh Rangel,[1,2]

Brett A. Helms,[1,4] Jeffrey R. Long,[3,4,5] and Jeffrey B. Neaton[1,2,6]*

[1]Molecular Foundry, Lawrence Berkeley National Laboratory, Berkeley, California 94720, USA

[2]Department of Physics, University of California, Berkeley, California 94720, USA

[3]Department of Chemistry, University of California, Berkeley, California 94720, USA

[4]Materials Sciences Division, Lawrence Berkeley National Laboratory, Berkeley, California 94720, USA

[5]Department of Chemical and Biomolecular Engineering, University of California, Berkeley, California 94720, USA

[6]Kavli Energy Nanosciences Institute at Berkeley, Berkeley, California 94720, USA

To whom correspondence should be addressed.

Email: jbneaton@lbl.gov

1. UV Measurements and Computed Band Gaps

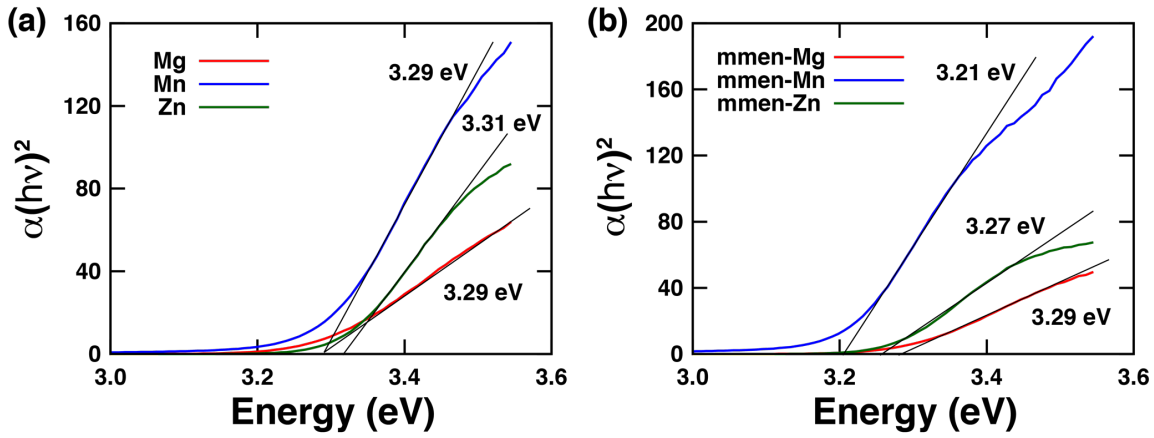

Fig. S1 Experimentally derived band gaps for (a) M_2(dobpdc) and (b) mmen−M_2(dobpdc) (M = Mg, Mn, Zn). Using the measured reflectance (R) from UV-Vis Diffusion Reflectance measurements, the extinction coefficient α is to be proportional to F(R), being F(R) = $(1-R^2)/2R$. Considering direct allowed transitions, we have $\alpha(h\nu)^2 \approx k(h\nu - Eg)$, where *h* is the Plank constant, *v* is the photon frequency, k is a the absorption constant, *Eg* is the band-gap energy (eV). Plotting $\alpha(h\nu)^2$ versus the photon energy, we extrapolated *Eg* fitting the slope and intersecting it with α = 0.[1]

(1) UV-Vis Diffuse Reflectance Measurements

Experimental optical band gaps are determined from diffuse reflectance measurements performed on bulk (powder) MOF samples. M_2(dobpdc) samples with different metal centers (M) are synthesized following a rapid route that we recently reported.[2] For amine-grafted samples, the M_2(dobpdc) powder is appended with mmen in hexanes prior to activation.[2] Freshly activated samples are loaded into an integrating sphere to perform the diffuse reflectance measurements on a Cary 5000 spectrophotometer. Spectra are acquired in the photon wavelength range 350 to 700 nm. Optical band gaps are determined from the experimental data according to a fitting procedure reported in literature for direct band-gap semiconductor materials, as shown in Fig S1.[1]

(2) HSE calculations

All computed band gaps are generated from single-point calculations with the HSE06[3] hybrid functional. HSE06 uses a fraction Fock short-range exact exchange (α) set to 0.25. For all HSE06 calculations, a 2 × 2 × 3 Monkhorst-Pack *k*-point mesh[4] centered at Γ is used. We also investigate the electronic structure of a H_4dobpdc molecule within a 17 Å × 20 Å × 16 Å supercell using HSE06.

Although the HSE functional does not include electron-hole interactions and is missing important nonlocal correlation effects, the computed band gaps are in good agreement with the measured optical band gaps, as compared in Table S1. It is worth mentioning that the experimentally-measured band gaps are the optical band gaps. In order to accurately predict the quasiparticle or optical gap, we would need an excited-state formalism, such as many-body perturbation theory, e.g., within the GW approximation[5–10] and the Bethe-Salpeter equation approach.[7,11–15] The use of the HSE functional to approximate quasiparticle band gaps often leads to an underestimate.[16] At the same time, the exciton binding energies of porous materials such as MOFs are expected to be large because the valence band maximum (VBM) and conduction band minimum (CBM) states of MOFs are spatially localized on the same subunit of the structure (see Fig. S2). Electron-hole interactions are much stronger in MOFs than in inorganic systems due to reduced screening, and thus the optical band gaps are expected to be much smaller than the quasiparticle band gaps in porous MOFs. Since the HSE functional does not account for electron-hole interactions, and since it typically underestimates the quasiparticle gap, the resultant cancellation of the errors very plausibly leads to fortuitous agreement with experiment in this case.

Table S1 Computed band gaps *Eg* (in eV) of M_2(dobpdc), mmen−M_2(dobpdc), and CO_2−mmen−M_2(dobpdc) (M = Mg, Mn, Fe, Co, Zn) compared to the experimental values.

	Eg of GGA+U	*Eg* of HSE	*Eg* of Exp
Mg	2.49	3.55	3.29
mmen–Mg	2.68	3.66	3.29
CO_2–mmen–Mg	2.37	3.29	-
Mn	2.46	3.48	3.29
mmen–Mn	2.45	3.29	3.21
CO_2–mmen–Mn	2.31	3.09	-
Fe	2.49	3.17	-
mmen–Fe	2.47	2.97	-
CO_2–mmen–Fe	2.29	2.79	-
Co	2.47	3.21	-
mmen–Co	2.61	3.42	-
CO_2–mmen–Co	2.31	3.20	-
Zn	2.62	3.68	3.31
mmen–Zn	2.56	3.55	3.27
CO_2–mmen–Zn	2.50	3.49	-

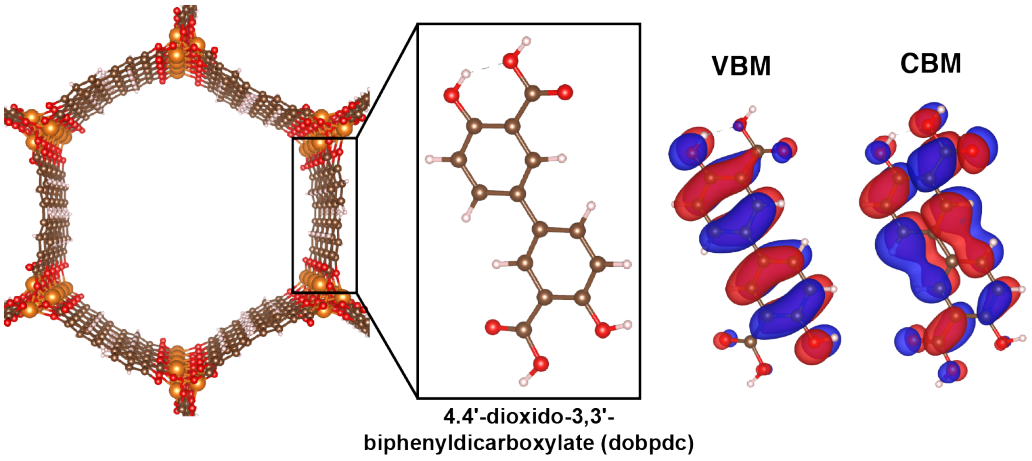

Fig. S2 4,4′-dioxidobiphenyl-3,3′-dicarboxylate (dobpdc) linker which is mainly responsible for the band edge states in M_2(dobpdc) MOFs.

2. Computed Kohn-Sham Energies

Table S2 Computed Kohn-Sham energies (in eV) of all metal-organic frameworks (MOFs) and free molecules.

MOF	Kohn-Sham energy	Molecule	Kohn-Sham energy
Mg_2(dobpdc)	-493.916	CO_2	-17.660
mmen–Mg_2(dobpdc)	-1028.408	H_2O	-12.481
CO_2–mmen–Mg_2(dobpdc)	-1139.015	N_2	-13.427
Mn_2(dobpdc)	-502.895	mmen	-87.526
mmen–Mn_2(dobpdc)	-1036.976	CO_2-mmen	-102.961
CO_2–mmen–Mn_2(dobpdc)	-1147.245		
Fe_2(dobpdc)	-492.110		
mmen–Fe_2(dobpdc)	-1026.795		
CO_2–mmen–Fe_2(dobpdc)	-1136.254		
Co_2(dobpdc)	-481.891		
mmen–Co_2(dobpdc)	-1016.633		
CO_2–mmen–Co_2(dobpdc)	-1125.856		
Zn_2(dobpdc)	-461.046		
mmen–Zn_2(dobpdc)	-994.835		
CO_2–mmen–Zn_2(dobpdc)	-1104.677		

3. Computed Vibrational Frequencies

Table S3 Computed vibrational frequencies for free (ν) and bound (ν') molecules. The unit is cm^{-1}.

Molecule	Mode	ν	ν'				
			Mg	Mn	Fe	Co	Zn
CO_2	1	2295	2299	2289	2288	2288	2286
	2	1291	1290	1287	1287	1287	1286
	3	623	617	613	611	612	613
	4	623	607	611	608	609	611
	5		148	121	139	130	115
	6		105	85	93	86	74
	7		83	80	81	75	61
	8		31	44	56	44	13
	9		4	28	38	29	19*i*
H_2O	1	3758	3737	3732	3724	3732	3731
	2	3658	3643	3634	3625	3632	3628
	3	1636	1619	1613	1613	1607	1612
	4		469	445	461	479	431
	5		385	375	411	417	373
	6		210	194	196	197	164
	7		128	108	109	112	114
	8		112	81	75	98	96
	9		61	37	56	69	79
N_2	1	2554	2417	2411	2409	2406	2407
	2		164	107	133	132	87
	3		143	96	118	114	77
	4		101	83	87	72	59
	5		33	22	33	28	24
	6		28	9	11*i*	28*i*	12*i*
mmen	1	3368	3383	3401	3380	3378	3395
($C_4H_{10}N_2H_2$)	2	3121	3100	3091	3086	3073	3308
	3	3055	3072	3073	3073	3059	3068
	4	3034	3055	3028	3044	3045	3042
	5	3014	3025	3007	3026	3023	3032
	6	3006	3006	2997	3009	3006	3023
	7	2986	3003	2986	2995	2998	2989
	8	2973	2974	2966	2974	2977	2983
	9	2970	2972	2941	2971	2972	2972
	10	2907	2919	2914	2917	2920	2953
	11	2900	2909	2896	2915	2913	2944
	12	2857	2868	2857	2862	2864	2849
	13	1512	1512	1513	1512	1512	1508
	14	1508	1503	1502	1504	1507	1506
	15	1500	1497	1496	1500	1501	1497
	16	1489	1492	1493	1491	1492	1489

	17	1483	1482	1485	1483	1485	1481
	18	1480	1482	1480	1481	1481	1478
	19	1474	1469	1475	1471	1473	1471
	20	1468	1464	1467	1462	1463	1461
	21	1444	1440	1441	1440	1440	1445
	22	1434	1437	1434	1437	1436	1437
	23	1384	1386	1381	1387	1388	1382
	24	1332	1338	1336	1337	1340	1363
	25	1319	1334	1328	1333	1333	1305
	26	1274	1281	1280	1282	1283	1263
	27	1204	1212	1210	1211	1215	1203
	28	1144	1194	1202	1191	1200	1178
	29	1135	1139	1141	1139	1140	1140
	30	1115	1124	1130	1125	1128	1128
	31	1074	1078	1080	1078	1079	1072
	32	1028	1059	1062	1064	1074	1045
	33	1009	1025	1042	1030	1031	1019
	34	983	992	1010	999	1001	990
	35	917	951	943	951	956	955
	36	900	916	906	915	918	921
	37	820	844	847	849	851	849
	38	769	786	790	786	786	794
	39	714	743	755	749	756	714
	40	503	525	532	527	535	565
	41	404	429	428	425	432	428
	42	346	412	404	416	422	386
	43	307	339	347	343	347	320
	44	252	259	284	265	270	254
	45	230	244	244	248	255	226
	46	143	203	193	205	217	219
	47	124	187	180	179	189	189
	48	63	168	162	163	173	168
	49		142	159	145	149	142
	50		123	130	124	130	108
	51		92	108	94	98	88
	52		83	69	80	83	75
	53		63	54	62	68	55
	54		48	36	38	53	38
CO_2–mmen	1	3112	3094	3093	3091	3090	3093
($C_4H_{10}N_2H_2CO_2$)	2	3089	3075	3077	3078	3077	3071
	3	3071	3058	3058	3067	3056	3050
	4	3068	3056	3037	3052	3045	3038
	5	3038	3043	3023	3039	3036	3020
	6	3011	3017	3017	3018	3020	2995
	7	2995	2987	2987	2989	2987	2980
	8	2982	2973	2982	2978	2978	2974

9	2956	2969	2973	2973	2973	2971
10	2935	2958	2966	2966	2968	2950
11	2897	2918	2918	2916	2915	2916
12	2707	2454	2503	2448	2465	2594
13	1645	1678	1678	1676	1676	1676
14	1503	1567	1563	1567	1568	1561
15	1500	1504	1504	1503	1504	1506
16	1495	1500	1500	1500	1500	1500
17	1491	1489	1491	1490	1490	1491
18	1487	1486	1485	1485	1486	1486
19	1468	1484	1483	1483	1483	1485
20	1450	1479	1479	1477	1479	1482
21	1438	1474	1473	1472	1472	1475
22	1429	1457	1455	1453	1453	1453
23	1402	1441	1439	1439	1440	1440
24	1374	1426	1420	1418	1417	1413
25	1367	1399	1397	1396	1398	1396
26	1339	1365	1358	1359	1360	1361
27	1320	1338	1336	1335	1336	1332
28	1302	1318	1315	1314	1314	1314
29	1257	1264	1264	1261	1261	1263
30	1180	1223	1217	1216	1215	1212
31	1172	1210	1208	1210	1209	1208
32	1157	1168	1165	1167	1168	1170
33	1129	1135	1131	1132	1132	1133
34	1082	1112	1108	1108	1109	1110
35	1013	1039	1036	1037	1036	1036
36	995	1015	1010	1013	1015	1014
37	962	1004	999	1000	1001	1000
38	955	973	970	973	975	976
39	889	933	940	932	932	936
40	856	914	911	914	916	914
41	783	816	811	811	811	812
42	755	781	779	779	779	782
43	749	761	759	761	761	760
44	598	628	626	626	627	624
45	558	578	573	574	574	572
46	410	458	452	455	458	453
47	387	419	421	419	420	415
48	349	384	375	377	379	373
49	279	323	318	321	323	322
50	250	287	282	282	285	283
51	188	250	248	248	250	253
52	181	231	226	220	223	226
53	137	218	209	210	212	210
54	111	172	161	164	170	170

55	86	151	141	143	144	147
56	34	131	123	125	129	127
57	5	124	118	118	119	119
58		109	104	103	105	104
59		104	94	96	97	94
60		78	66	63	70	70
61		59	52	55	54	64
62		52	48	43	50	50
63		46	36	41	35	47

Table S4 Computed vibrational frequencies of bound H_2O in Mg_2(dobpdc) for different kinetic energy cutoffs (KE), force criteria (F), and convergence thresholds for self-consistency (CT). The unit is cm^{-1}. Imaginary frequencies are indicated by red.

Mode	KE: 600 eV F: 0.02 eV/Å CT: 10^{-5} eV	600 eV 0.01 eV/Å 10^{-5} eV	1000 eV 0.02 eV/Å 10^{-5} eV	1000 eV 0.01 eV/Å 10^{-5} eV	600 eV 0.02 eV/Å 10^{-8} eV
1	3737	3734	3742	3743	3737
2	3643	3640	3651	3652	3643
3	1605	1606	1599	1598	1619
4	444	426	417	414	469
5	370	347	364	358	385
6	206	203	198	195	210
7	118	63	112	110	128
8	66*i*	135*i*	80*i*	85*i*	112
9	214*i*	265*i*	211*i*	211*i*	61

4. Zero-Point and Thermal Energy Corrections

(1) Zero-point energy

Due to the uncertainty principles, small gas molecules fluctuate even at 0 K. This quantum mechanical behavior increases the ground state energy by $\hbar\omega_{vib}/2$ where $\hbar$ is Planck's constant divided by 2π, and ω_{vib} is the vibrational frequency. Therefore, in order to accurately predict binding energies of small gas molecules, we need to consider zero-point energy (ZPE) and add this number to the calculated Kohn-Sham energy. The total ZPE contribution can be expressed as

$$ZPE = \sum_{vib} \frac{\hbar\omega_{vib}}{2} . \quad (9)$$

The ZPE correction (ZPEC) can be then obtained via the difference between the ZPEs of free and bound molecules.

$$ZPEC = \sum_{vib,bound} \frac{\hbar\omega_{vib,bound}}{2} - \sum_{vib,free} \frac{\hbar\omega_{vib,free}}{2} . \quad (10)$$

Using the computed vibrational frequencies of free and bound molecules given in Table S2, we can get the ZPEC for all molecules as shown in Table S4.

Table S5 Computed ZPEC (in kJ/mol) for CO_2, H_2O, N_2, mmen, and CO_2–mmen molecules.

	Mg	Mn	Fe	Co	Zn
CO_2	2.1	2.0	2.2	2.0	1.5
H_2O	7.9	7.0	7.3	7.7	7.0
N_2	2.0	1.0	1.4	1.4	0.7
mmen	7.8	7.4	7.7	8.6	8.6
CO_2–mmen	10.7	9.7	9.6	9.9	10.1

(2) Thermal energy

The thermal energy (TE) correction arises from with the internal kinetic energy caused by the random motion of free molecules including vibrational, translational, and rotational degrees of freedom. Thus, TE correction is proportional to the temperature and can be expressed as

$$TE_{free}(T) = \sum_{trans,rot} \frac{1}{2} k_B T + \sum_{vib} \frac{\hbar\omega_{vib}}{e^{\frac{\hbar\omega_{vib}}{k_B T}} - 1} \quad (11)$$

where k_B is Boltzmann constant, and T is the temperature. For the bound molecules, the TE is

$$TE_{bound}(T) = \sum_{vib} \frac{\hbar\omega_{vib}}{e^{\frac{\hbar\omega_{vib}}{k_B T}} - 1} \quad (12)$$

since the translational and rotational degrees of freedom are no longer applicable. Then the TE correction (TEC) is calculated as:

$$TEC(T) = TE_{bound}(T) - TE_{free}(T) \quad (13)$$

Using the computed vibrational frequencies of free and bound molecules given in Table S2, we can get the TEC for all molecules as shown in Table S5.

Table S6 Computed TEC (in kJ/mol) for CO_2, H_2O, N_2, mmen, and CO_2–mmen molecules.

	Mg	Mn	Fe	Co	Zn
CO_2	1.7	1.8	1.5	1.7	2.2
H_2O	-1.2	-0.7	-0.9	-1.1	-0.8
N_2	1.2	2.0	1.6	1.7	2.3
mmen	0.2	0.3	0.3	-0.1	0.6
CO_2–mmen	-0.9	-0.4	-0.4	-0.6	-0.6

5. Mechanical Properties

(1) Voigt-Reuss-Hill (VRH) average

The orientationally-averaged Young's modulus *E*, bulk moduls *B*, shear modulus *G*, and Poisson's ratio *v* can be estimated using the VRH average.[17]

$$B_V = \frac{1}{9}[(C_{11} + C_{22} + C_{33}) + 2(C_{12} + C_{13} + C_{23})] \quad (1)$$

$$B_R = \frac{1}{(S_{11}+S_{22}+S_{33})+2(S_{12}+S_{13}+S_{23})} \quad (2)$$

$$G_V = \frac{1}{15}[(C_{11} + C_{22} + C_{33}) - (C_{12} + C_{13} + C_{23}) + 3(C_{44} + C_{55} + C_{66})] \quad (3)$$

$$G_R = \frac{15}{4(S_{11}+S_{22}+S_{33})-4(S_{12}+S_{13}+S_{23})+3(S_{44}+S_{55}+S_{66})} \quad (4)$$

$$B = B_{VRH} = \frac{B_R+B_V}{2} \quad (5)$$

$$G = G_{VRH} = \frac{G_R+G_V}{2} \quad (6)$$

$$E = E_{VRH} = \frac{9B_{VRH}G_{VRH}}{3B_{VRH}+G_{VRH}} \quad (7)$$

$$\nu = \nu_{VRH} = \frac{3B_{VRH}-2G_{VRH}}{6B_{VRH}+2G_{VRH})} \quad (8)$$

where subscript V and R indicate the Voigt and Reuss average[18,19] by which the orientationally-averaged bulk modulus can be determined, indicating the upper and lower bound of the modulus for a polycrystalline material.

(2) Two strain types

Two different strain types (ε_1 and ε_{3+4}) were calculated for M_2(dobpdc), mmen-M_2(dobpdc), and CO_2-mmen-M_2(dobpdc) (M = Mg, Mn, Fe, Co, Zn). δ indicates a strain.

$$\varepsilon_1 = \begin{bmatrix} 1+\delta & 0 & 0 \\ 0 & 1 & 0 \\ 0 & 0 & 1 \end{bmatrix}$$

$$\varepsilon_{3+4} = \begin{bmatrix} 1 & 0 & 0 \\ 0 & 1 & \delta/2 \\ 0 & \delta/2 & 1+\delta \end{bmatrix}$$

(3) Elastic moduli (C_{ij})

$$C_{ij}[Mg_2(dobpdc)] = \begin{bmatrix} 15.96 & 13.93 & 3.84 & 0 & 0 & 0 \\ 13.93 & 15.96 & 3.84 & 0 & 0 & 0 \\ 3.84 & 3.84 & 17.01 & 0 & 0 & 0 \\ 0 & 0 & 0 & 6.35 & 0 & 0 \\ 0 & 0 & 0 & 0 & 6.35 & 0 \\ 0 & 0 & 0 & 0 & 0 & 1.02 \end{bmatrix}$$

$$C_{ij}[Mn_2(dobpdc)] = \begin{bmatrix} 19.97 & 19.23 & 6.47 & 0 & 0 & 0 \\ 19.23 & 19.97 & 6.47 & 0 & 0 & 0 \\ 6.47 & 6.47 & 13.19 & 0 & 0 & 0 \\ 0 & 0 & 0 & 5.59 & 0 & 0 \\ 0 & 0 & 0 & 0 & 5.59 & 0 \\ 0 & 0 & 0 & 0 & 0 & 0.37 \end{bmatrix}$$

$$C_{ij}[Fe_2(dobpdc)] = \begin{bmatrix} 16.98 & 14.87 & 3.66 & 0 & 0 & 0 \\ 14.87 & 16.98 & 3.66 & 0 & 0 & 0 \\ 3.66 & 3.66 & 13.19 & 0 & 0 & 0 \\ 0 & 0 & 0 & 5.93 & 0 & 0 \\ 0 & 0 & 0 & 0 & 5.93 & 0 \\ 0 & 0 & 0 & 0 & 0 & 1.06 \end{bmatrix}$$

$$C_{ij}[Co_2(dobpdc)] = \begin{bmatrix} 13.69 & 12.85 & 2.90 & 0 & 0 & 0 \\ 12.85 & 13.69 & 2.90 & 0 & 0 & 0 \\ 2.90 & 2.90 & 13.19 & 0 & 0 & 0 \\ 0 & 0 & 0 & 6.34 & 0 & 0 \\ 0 & 0 & 0 & 0 & 6.34 & 0 \\ 0 & 0 & 0 & 0 & 0 & 0.42 \end{bmatrix}$$

$$C_{ij}[Zn_2(dobpdc)] = \begin{bmatrix} 16.93 & 15.55 & 5.33 & 0 & 0 & 0 \\ 15.55 & 16.93 & 5.33 & 0 & 0 & 0 \\ 5.33 & 5.33 & 12.42 & 0 & 0 & 0 \\ 0 & 0 & 0 & 5.21 & 0 & 0 \\ 0 & 0 & 0 & 0 & 5.93 & 0 \\ 0 & 0 & 0 & 0 & 0 & 0.69 \end{bmatrix}$$

$$C_{ij}[mmen - Mg_2(dobpdc)] = \begin{bmatrix} 17.20 & 10.66 & 4.58 & 0 & 0 & 0 \\ 10.66 & 17.20 & 4.58 & 0 & 0 & 0 \\ 4.58 & 4.58 & 20.54 & 0 & 0 & 0 \\ 0 & 0 & 0 & 7.57 & 0 & 0 \\ 0 & 0 & 0 & 0 & 7.57 & 0 \\ 0 & 0 & 0 & 0 & 0 & 3.27 \end{bmatrix}$$

$$C_{ij}[mmen - Mn_2(dobpdc)] = \begin{bmatrix} 20.09 & 15.78 & 2.79 & 0 & 0 & 0 \\ 15.78 & 20.09 & 2.79 & 0 & 0 & 0 \\ 2.79 & 2.79 & 15.69 & 0 & 0 & 0 \\ 0 & 0 & 0 & 4.81 & 0 & 0 \\ 0 & 0 & 0 & 0 & 4.81 & 0 \\ 0 & 0 & 0 & 0 & 0 & 2.15 \end{bmatrix}$$

$$C_{ij}[mmen - Fe_2(dobpdc)] = \begin{bmatrix} 17.93 & 11.02 & 3.60 & 0 & 0 & 0 \\ 11.02 & 17.93 & 3.60 & 0 & 0 & 0 \\ 3.60 & 3.60 & 15.68 & 0 & 0 & 0 \\ 0 & 0 & 0 & 7.05 & 0 & 0 \\ 0 & 0 & 0 & 0 & 7.05 & 0 \\ 0 & 0 & 0 & 0 & 0 & 3.45 \end{bmatrix}$$

$$C_{ij}[mmen - Co_2(dobpdc)] = \begin{bmatrix} 12.40 & 9.09 & 2.65 & 0 & 0 & 0 \\ 9.09 & 12.40 & 2.65 & 0 & 0 & 0 \\ 2.65 & 2.65 & 20.61 & 0 & 0 & 0 \\ 0 & 0 & 0 & 7.00 & 0 & 0 \\ 0 & 0 & 0 & 0 & 7.00 & 0 \\ 0 & 0 & 0 & 0 & 0 & 1.65 \end{bmatrix}$$

$$C_{ij}[mmen - Zn_2(dobpdc)] = \begin{bmatrix} 20.58 & 13.45 & 6.70 & 0 & 0 & 0 \\ 13.45 & 20.58 & 6.70 & 0 & 0 & 0 \\ 6.70 & 6.70 & 22.75 & 0 & 0 & 0 \\ 0 & 0 & 0 & 6.86 & 0 & 0 \\ 0 & 0 & 0 & 0 & 6.86 & 0 \\ 0 & 0 & 0 & 0 & 0 & 3.56 \end{bmatrix}$$

$$C_{ij}[CO_2 - mmen - Mg_2(dobpdc)] = \begin{bmatrix} 21.46 & 15.27 & 6.65 & 0 & 0 & 0 \\ 15.27 & 21.46 & 6.65 & 0 & 0 & 0 \\ 6.65 & 6.65 & 30.57 & 0 & 0 & 0 \\ 0 & 0 & 0 & 9.50 & 0 & 0 \\ 0 & 0 & 0 & 0 & 9.50 & 0 \\ 0 & 0 & 0 & 0 & 0 & 3.10 \end{bmatrix}$$

$$C_{ij}[CO_2 - mmen - Mn_2(dobpdc)] = \begin{bmatrix} 20.99 & 12.59 & 8.48 & 0 & 0 & 0 \\ 12.59 & 20.99 & 8.48 & 0 & 0 & 0 \\ 8.48 & 8.48 & 22.04 & 0 & 0 & 0 \\ 0 & 0 & 0 & 7.48 & 0 & 0 \\ 0 & 0 & 0 & 0 & 7.48 & 0 \\ 0 & 0 & 0 & 0 & 0 & 1.06 \end{bmatrix}$$

$$C_{ij}[CO_2 - mmen - Fe_2(dobpdc)] = \begin{bmatrix} 18.85 & 14.05 & 8.51 & 0 & 0 & 0 \\ 14.05 & 18.85 & 8.51 & 0 & 0 & 0 \\ 8.51 & 8.51 & 28.50 & 0 & 0 & 0 \\ 0 & 0 & 0 & 7.92 & 0 & 0 \\ 0 & 0 & 0 & 0 & 7.92 & 0 \\ 0 & 0 & 0 & 0 & 0 & 2.40 \end{bmatrix}$$

$$C_{ij}[CO_2 - mmen - Co_2(dobpdc)] = \begin{bmatrix} 18.64 & 13.01 & 7.58 & 0 & 0 & 0 \\ 13.01 & 18.64 & 7.58 & 0 & 0 & 0 \\ 7.58 & 7.58 & 28.25 & 0 & 0 & 0 \\ 0 & 0 & 0 & 8.95 & 0 & 0 \\ 0 & 0 & 0 & 0 & 8.95 & 0 \\ 0 & 0 & 0 & 0 & 0 & 2.82 \end{bmatrix}$$

$$C_{ij}[CO_2 - mmen - Zn_2(dobpdc)] = \begin{bmatrix} 22.81 & 15.93 & 10.22 & 0 & 0 & 0 \\ 15.93 & 22.81 & 10.22 & 0 & 0 & 0 \\ 10.22 & 10.22 & 20.70 & 0 & 0 & 0 \\ 0 & 0 & 0 & 7.07 & 0 & 0 \\ 0 & 0 & 0 & 0 & 7.07 & 0 \\ 0 & 0 & 0 & 0 & 0 & 3.44 \end{bmatrix}$$

6. Disordered mmen and CO_2–mmen units

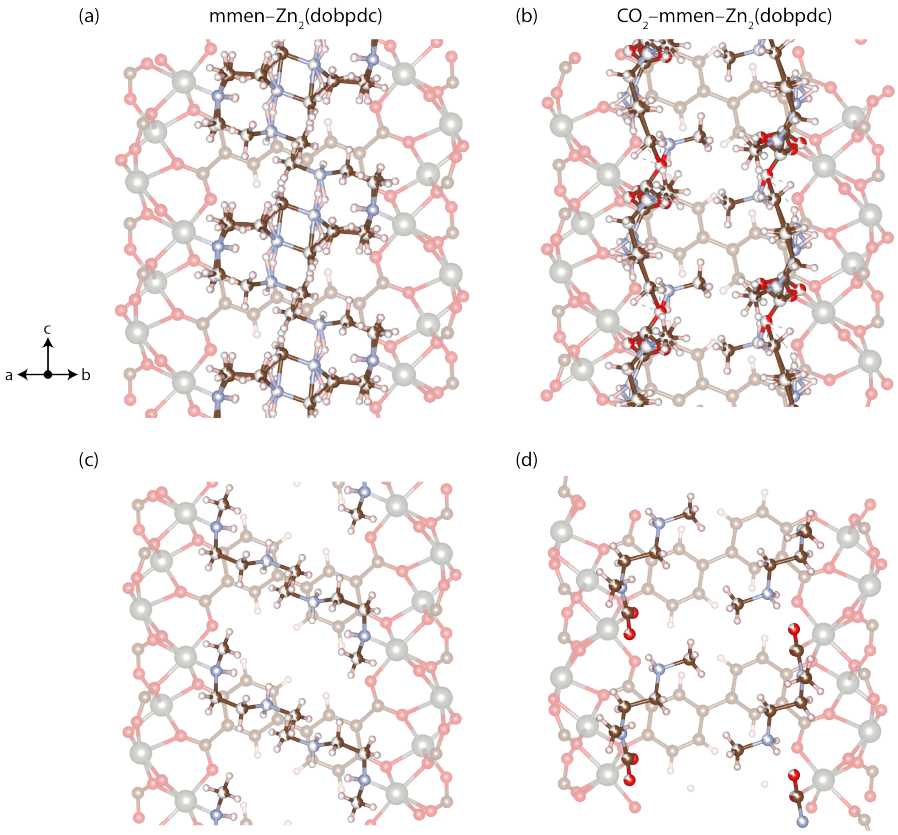

Fig. S3 Experimentally-determined X-ray diffraction crystal structures of (a) mmen–Zn_2(dobpdc) and (b) CO_2–mmen–Zn_2(dobpdc). mmen and CO_2–mmen units are disordered. Possible (c) mmen and (d) CO_2–mmen orderings in mmen–Zn_2(dobpdc) and CO_2–mmen–Zn_2(dobpdc).

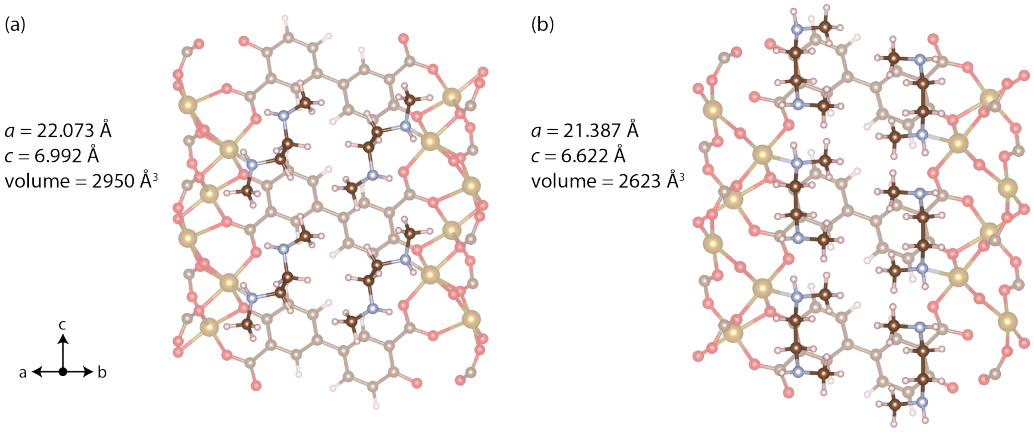

Fig. S4 Two different mmen orderings in mmen–Fe_2(dobpdc) with different optimized lattice parameters and unit cell volumes. A structure in (b) is obtained from the previous *ab-initio* molecular dynamics studies.[20,21]

7. Powder diffraction patterns

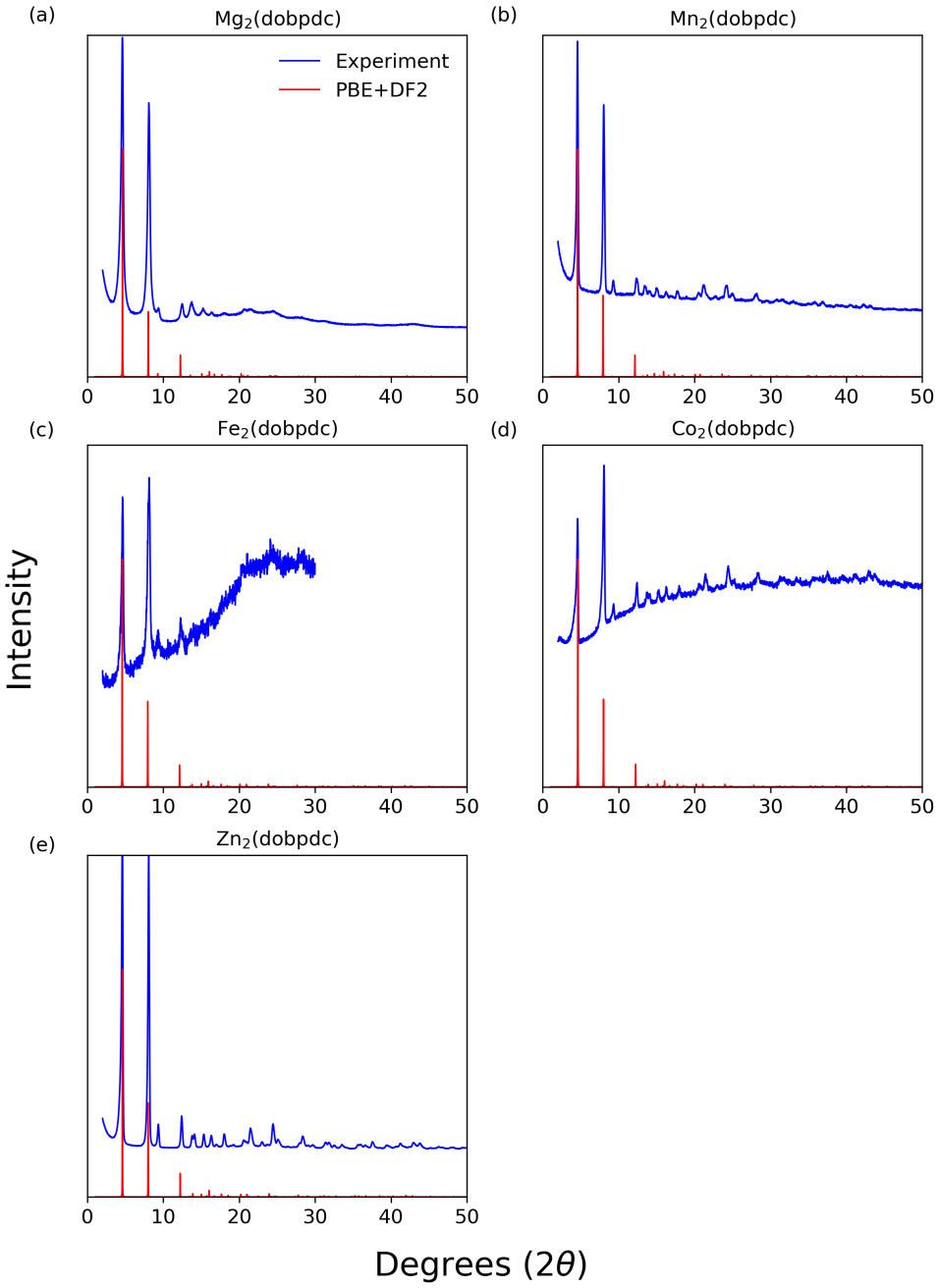

Fig. S5 Powder diffraction patterns of the optimized (a) Mg_2(dobpdc), (b) Mn_2(dobpdc), (c) Fe_2(dobpdc), (d) Co_2(dobpdc), and (e) Zn_2(dobpdc) structures compared to the experimental powder diffractions collected at 298 K with λ = 1.5418 Å.[22] The experimental curves (blue curves) are taken from Ref. 22.

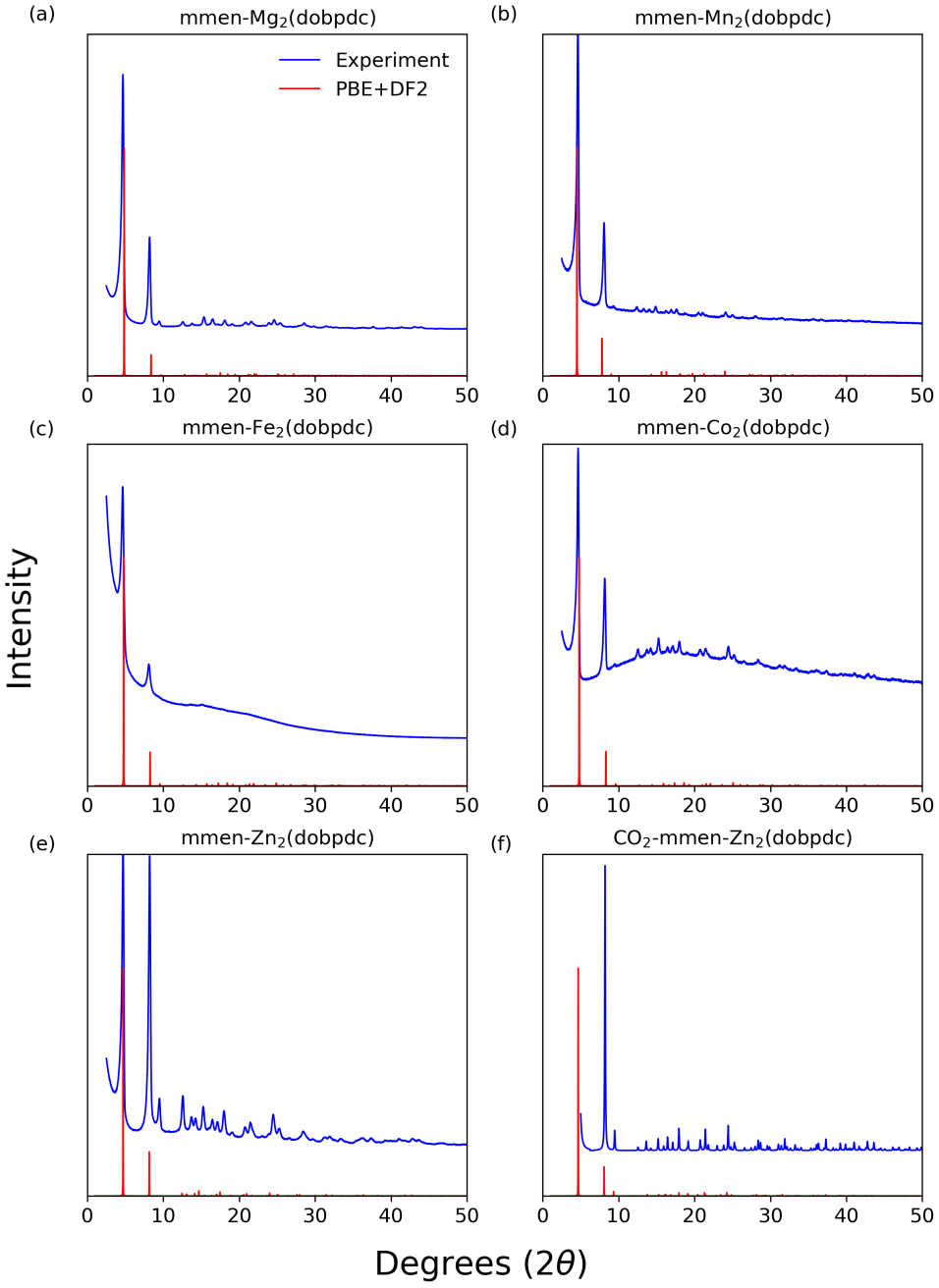

Fig. S6 Powder diffraction patterns of the optimized (a) mmen–Mg_2(dobpdc), (b) mmen–Mn_2(dobpdc), (c) mmen–Fe_2(dobpdc), (d) mmen–Co_2(dobpdc), (e) mmen–Zn_2(dobpdc), and (f) CO_2–mmen–Zn_2(dobpdc) structures compared to the experimental powder diffractions collected at 298 K with λ = 1.5406 Å.[20,23] The experimental curves (blue curves) are taken from Ref. 20 and 23.

8. Potential curves

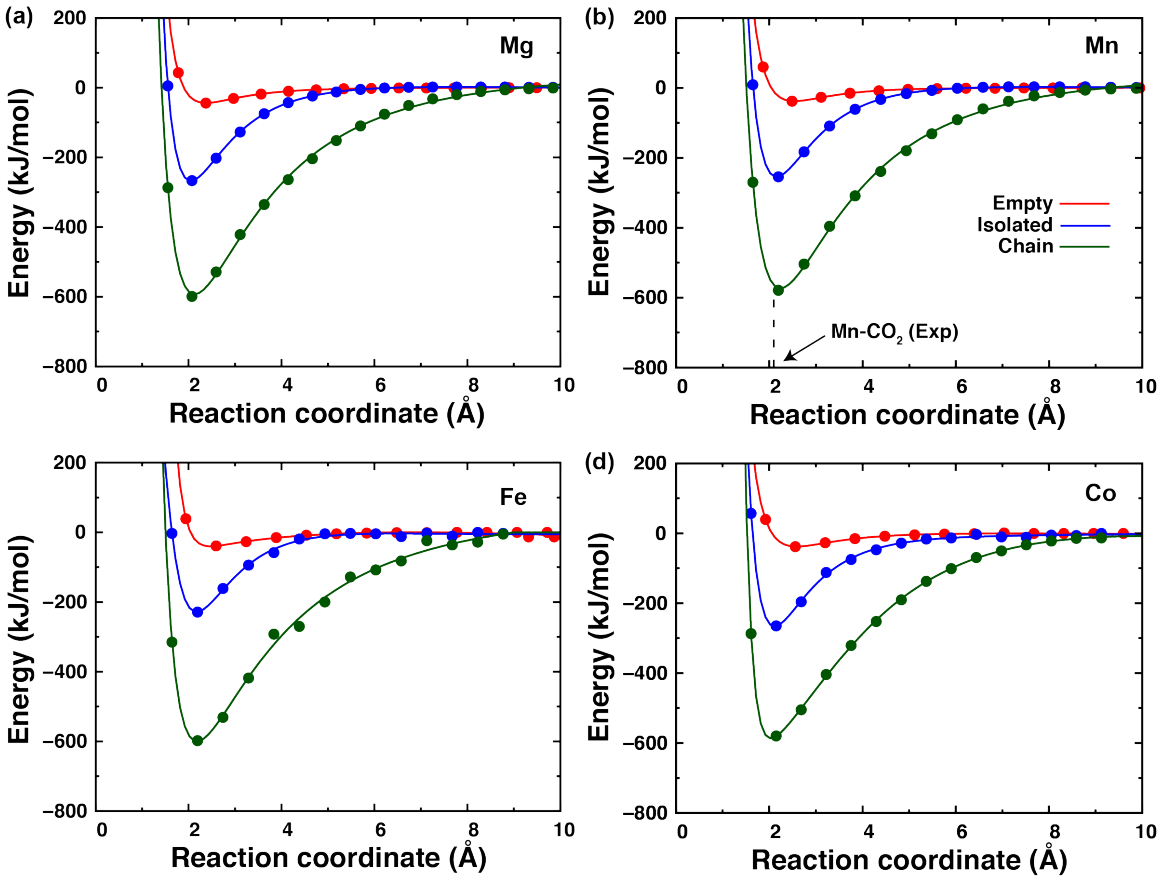

Fig S7 Potential curves of Empty, Isolated, and Chain geometries for (a) Mg_2(dobpdc), (b) Mn_2(dobpdc), (c) Fe_2(dobpdc), and (d) Co_2(dobpdc). The experimental Mn–CO_2 distance is indicated by the dotted line.

9. Charge Density Difference ($\Delta\rho$) for CO_2 in Zn_2(dobpdc)

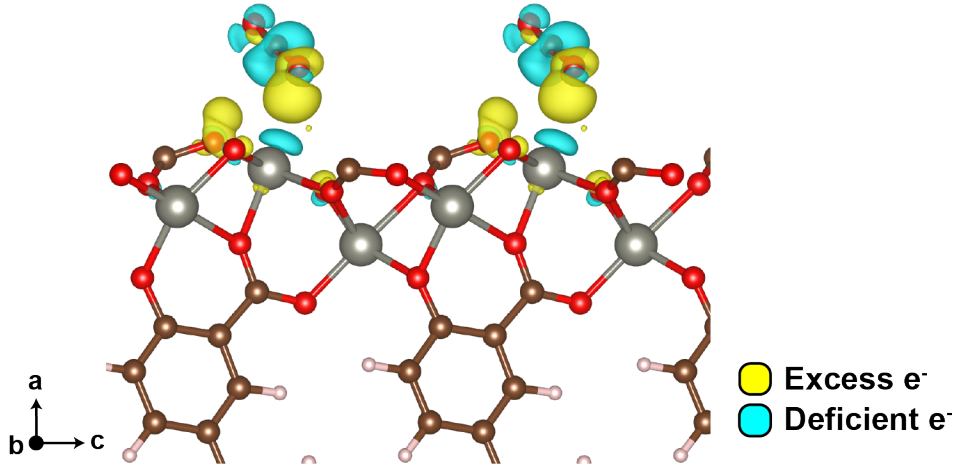

Fig S8 Isosurface plot of the charge density difference ($\Delta\rho$) for the CO_2 in the Empty geometry. The isosurface level is equal to 0.005 e/Å^3.

References

1 R. López and R. Gómez, *J. Sol-Gel Sci. Technol.*, 2012, **61**, 1–7.
2 L. Maserati, S. M. Meckler, C. Li and B. A. Helms, *Chem. Mater.*, 2016, **28**, 1581–1588.
3 J. Heyd, G. E. Scuseria and M. Ernzerhof, *J. Chem. Phys.*, 2003, **118**, 8207–8215.
4 J. D. Pack and H. J. Monkhorst, *Phys. Rev. B*, 1977, **16**, 1748–1749.
5 L. Hedin, *Phys. Rev.*, 1965, **139**, A796.
6 G. Strinati, H. J. Mattausch and W. Hanke, *Phys. Rev. Lett.*, 1980, **45**, 290–294.
7 G. Strinati, H. J. Mattausch and W. Hanke, *Phys. Rev. B*, 1982, **25**, 2867–2888.
8 M. S. Hybertsen and S. G. Louie, *Phys. Rev. B*, 1986, **34**, 5390–5413.
9 R. W. Godby, M. Schlüter and L. J. Sham, *Phys. Rev. B*, 1988, **37**, 10159–10175.
10 F. Aryasetiawan and O. Gunnarsson, *Reports Prog. Phys.*, 1998, **61**, 237–312.
11 L. J. Sham and T. M. Rice, *Phys. Rev.*, 1966, **144**, 708–714.
12 W. Hanke and L. Sham, *Phys. Rev. Lett.*, 1979, **43**, 387–390.
13 M. Rohlfing and S. Louie, *Phys. Rev. Lett.*, 1998, **80**, 3320–3323.
14 L. X. Benedict, E. L. Shirley and R. B. Bohn, *Phys. Rev. Lett.*, 1998, **80**, 4514.
15 S. Albrecht, L. Reining, R. Del Sole and G. Onida, *Phys. Rev. Lett.*, 1998, **80**, 4510–4513.
16 F. Fuchs, J. Furthmüller, F. Bechstedt, M. Shishkin and G. Kresse, *Phys. Rev. B*, 2007, **76**, 115109.
17 R. Hill, *Proc. Phys. Soc. Sect. A*, 1952, **65**, 349–354.
18 A. Reuss, *ZAMM - Zeitschrift für Angew. Math. und Mech.*, 1929, **9**, 49–58.
19 W. Voigt, *Lehrbuch der Kristallphysik*, Teubner, 1966.
20 T. M. McDonald, J. A. Mason, X. Kong, E. D. Bloch, D. Gygi, A. Dani, V. Crocellà, F. Giordanino, S. O. Odoh, W. S. Drisdell, B. Vlaisavljevich, A. L. Dzubak, R. Poloni, S. K. Schnell, N. Planas, K. Lee, T. Pascal, L. F. Wan, D. Prendergast, J. B. Neaton, B. Smit, J. B. Kortright, L. Gagliardi, S. Bordiga, J. A. Reimer and J. R. Long, *Nature*, 2015, **519**, 303–308.
21 B. Vlaisavljevich, S. O. Odoh, S. K. Schnell, A. L. Dzubak, K. Lee, N. Planas, J. B. Neaton, L. Gagliardi and B. Smit, *Chem. Sci.*, 2015, **6**, 5177–5185.
22 D. Gygi, E. D. Bloch, J. A. Mason, M. R. Hudson, M. I. Gonzalez, R. L. Siegelman, T. A. Darwish, W. L. Queen, C. M. Brown and J. R. Long, *Chem. Mater.*, 2016, **28**, 1128–1138.
23 R. L. Siegelman, T. M. McDonald, M. I. Gonzalez, J. D. Martell, P. J. Milner, J. A. Mason, A. H. Berger, A. S. Bhown and J. R. Long, *J. Am. Chem. Soc.*, 2017, **139**, 10526–10538.